

Manuscript received December 18, 2023; revised January 20, 2024; accepted January 12, 2024; date of publication Mei 23, 2024

Digital Object Identifier (DOI): <https://doi.org/10.35882/ijeemi.v6i2.355>

Copyright © 2024 by the authors. This work is an open-access article and licensed under a Creative Commons Attribution-ShareAlike 4.0 International License ([CC BY-SA 4.0](https://creativecommons.org/licenses/by-sa/4.0/))

How to cite: Nyatte Steyve, Perabi Steve, Mepouly Kedy, Salomé Ndjakomo, Ele pierre, "A Hybrid Approach for Optimal Multi-Class Classification of Neglected Tropical Skin Diseases using Multi-Channel HOG Features", Indonesian Journal of Electronics, Electromedical Engineering, and Medical Informatics, vol. 6, no. 1, pp. 93-108, Mei. 2024.

A Hybrid Approach for Optimal Multi-Class Classification of Neglected Tropical Skin Diseases using Multi-Channel HOG Features

Nyatte Steyve^{1*}, Perabi Steve¹, Mepouly Kedy¹, Salomé Ndjakomo^{1,2}, Ele pierre^{1,3}

¹ Laboratory of Technology and Applied Sciences, University of Douala, Cameroon

² Signal, Image and Systems Laboratory, University of Yaounde, Cameroon

³ Laboratory of Electrical Engineering, Mechatronics and Signal Treatment, National Advanced School of Engineering, University of Yaoundé 1, Yaoundé, Cameroon

ABSTRACT Neglected tropical skin diseases (NTDs) pose significant health challenges, especially in resource-limited settings. Early diagnosis is crucial for effective treatment and preventing complications. This study proposes a novel multi-class classification approach using multi-channel HOG features and a hybrid metaheuristic algorithm to improve the accuracy of NTD diagnosis. The method extracts optimal HOG features from images of Buruli Ulcer, Leprosy, and Cutaneous Leishmaniasis through different cell sizes, generating multiple training datasets. A hybrid Whale Optimization Algorithm and Shark Smell Optimization Algorithm (WOA-SSO) optimizes the Error Correcting Output Code (ECOC) framework for SVM, achieving superior multi-class classification performance. Notably, the multi-channel dataset, derived from averaging HOG features of different cell sizes, yields the highest accuracy of 89%. This study demonstrates the potential of the proposed method for developing mobile applications that facilitate early and accurate diagnosis of NTDs through image analysis, potentially improving patient outcomes and disease control. The hybrid metaheuristic algorithm plays a crucial role in optimizing the ECOC framework, enhancing the accuracy and efficiency of the multi-class classification process. This approach holds significant promise for revolutionizing NTD diagnosis and management, particularly in underserved communities.

INDEX TERMS Multi-class Diagnosis, Optimal shape feature Extraction, Neglected tropical skin disease

I. INTRODUCTION

Neglected tropical skin diseases (NTDs) are a group of infectious diseases that primarily affect populations in low- and middle-income countries. These diseases cause significant morbidity and disability, impacting millions of people worldwide. NTDs often affect the skin and soft tissues, leading to disfigurement, social stigma, and economic hardship. According to the World Health Organization (WHO), NTDs affect over 1 billion people globally, with the majority of cases occurring in Africa, Asia, and Latin America. These diseases are often neglected due to poverty, lack of awareness, and inadequate healthcare infrastructure. The global impact of NTDs is substantial, contributing to poverty, social exclusion, and reduced productivity. The majority of these diseases affect very seriously the skin .

The skin is the most visible structural element, so any disease can have a considerable effect on the psychic, moral, and social levels. In the tropics, many human diseases lead to deep alterations of the skin that can lead to mutilation of limbs and irreversible deformations, which increases the feeling of isolation and stigmatization felt by the people who suffer from these conditions. Before reaching these extremes, symptoms range from changes in color, feel, or appearance. In fact, it is through these first signs that diseases are easily treated, often just with antibiotics. But unfortunately, the isolation of the endemic areas characterized by the lack of basic social facilities, well-trained personnel, and prevailing poverty does not favor early diagnosis. Current diagnostic methods for NTDs often lack sensitivity and specificity, leading to delayed diagnosis and suboptimal treatment outcomes. Traditional

methods rely on clinical examination and laboratory tests, which can be time-consuming, expensive, and require specialized expertise. Moreover, these methods may not be readily available in resource-limited settings.

Early detection is crucial for effective NTD management, as timely treatment can prevent complications and improve patient outcomes. However, the lack of accurate and accessible diagnostic tools poses a significant challenge in controlling these diseases. Therefore, there is a pressing need for improved early detection techniques that are accurate, affordable, and easy to implement in resource-constrained settings.

The Neglected Tropical Diseases (NTDs) studied here include Buruli Ulcer (BU), Leprosy (LEP), and cutaneous leishmaniasis (LEI), all of which cause significant skin changes at some stage of their evolution. Transmitted by *Mycobacterium Ulcerans*, Buruli ulcer is an infectious disease affecting mainly the skin of children under 15 years of age [1]. For the moment, its mode of transmission is unknown. However, its early form is characterized by the appearance of raised nodules that will later transform into a single, large ulcer with a yellowish surface and a moist, reddish base. Cutaneous leishmaniasis is an infection of the skin, affecting people of all ages, caused by a protozoan. The disease also presents as round or plaque-like skin nodules, the central part of which may ulcerate [2]. Like the previous ones, the first signs of leprosy are the appearance of skin patches or nodules of varying size. It is a systemic infectious disease that can occur at any age and is caused by a bacterium (*Mycobacterium leprae*). The current diagnosis of these diseases is very difficult in rural areas, and the current methods, which are all based on the identification of bacteria by microscopy, culture, and histopathology, have a sensitivity of less than 60% [3]. However, the ongoing development of image processing techniques and analysis by machine learning algorithms can help to develop effective and efficient tests, as for the diagnosis of various skin cancers [4-6], breast cancer [7-8], and lung cancer [9-10]. Works in this direction have been identified in the literature.

The detection of skin diseases in general based on images of skin lesions is being studied by many researchers in the fields of machine learning and artificial intelligence. Researchers have used various data mining, statistical, and machine learning algorithms in the literature. For example, neural networks and support vector machines (SVM) are widely used in skin cancer detection [11]. The authors of [12]

give a good overview of the different data mining techniques used for skin disease detection. However, we have noticed that very few are interested in the detection of neglected tropical skin diseases, even though this is basically a classification task like for cancer. Thus, the authors [13] combined skin images

and clinical data for the diagnosis of leprosy using a convolutional neural network (CNN). The best result was obtained with a high classification accuracy (90%) and an area under the curve (AUC) of 96.46%. The authors of [14] identified Buruli ulcer lesions from images through a Support Vector Machine (SVM). The limitation of this work is that the authors deal with images in the ulcer phase, which does not solve the problem of early detection of the disease. The authors of [15] diagnosed and prognosticated cutaneous leishmaniasis using artificial neural networks. The overall accuracy in terms of sensitivity, specificity and area under the ROC curve (AUC) of the Multilayer perceptron (MLP) classifier was 87.8%, 90.3%, 86% and 88%, respectively. In 2022, an artificial intelligence algorithm for the automatic detection of leishmaniasis from the parasite was developed with a recall of 65% and an accuracy of 50% [16]. The authors of [17] developed a neural network based leishmaniasis diagnostic system with 85.71% accuracy. The best results were obtained by neural networks, but these networks need to be deep to be effective and therefore require a large data set [18] and significant hardware and software resources. However, our database being limited, and knowing that SVMs give the best results on small datasets [19–20], this is the reason why it was requested by the authors of [14]. Nyatte et al [15] worked on the diagnosis of three neglected tropical diseases by optimizing an SVM with a black hole algorithm and obtained an accuracy above 96%. But the authors performed a ONE VS ALL classification, i.e., it was not a multi-class classification problem despite the fact that the authors worked on several diseases. However, the Error Correcting Code (ECOC) algorithm is widely used in the literature to solve multi-class classification problems of classical SVMs.

Among this research, none of them has considered an approach to address several skin NTDs at the same time when we know that these diseases have almost the same similarities in their initial phase. For us to propose a single diagnostic method will reduce the number of diagnostic hits. Table 1 summarizes the limitations of skin NTD research by machine learning.

TABLE 1: SUMMARIZING THE RESEARCH GAP

Reference	Diseases	Method	Limit (According to Us)
[14]	Buruli Ulcer	SVM	1. Late diagnosis (in the ulcer phase) Patients in this phase run away from the stigma by hiding. 2. Low accuracy and single disease diagnosis
[16]	Leishmaniasis	MLP	1.Diagnosis based on microscopic images of bacteria. Difficult to implement in the context of poor countries and endemic areas (Landlocked)

			2. Not sensitive enough and single disease diagnosis
[13]	Leprosy	CNN	single disease diagnosis
[15]	Buruli Ulcer, Leishmaniasis, Leprosy	BO-SVM	One Vs All Classification
Our proposal	Buruli Ulcer, Leishmaniasis, Leprosy	WOA-SSA-ECOC-SVM	Optimal Multi class classification scheme

The aim of this study is to propose an efficient and simple method to provide an optimal dataset and an optimized multi-class classification method for early diagnosis of neglected tropical skin diseases (NTDs) including Buruli Ulcer (BU), Leprosy, and Cutaneous Leishmaniasis using multi-channel HOG features and a hybrid metaheuristic algorithm. Histogram of Oriented Gradients (HOG) features are a powerful image descriptor that captures the shape and appearance of objects in an image. HOG features are based on the distribution of gradient orientations in local image patches. They are invariant to illumination changes and robust to geometric transformations, making them suitable for object detection and classification tasks. HOG features have been widely used in image classification, particularly in computer vision applications. Their ability to extract discriminative features from images makes them well-suited for classifying different types of objects. In the context of NTD diagnosis, HOG features can be used to identify characteristic patterns in skin lesion images, aiding in the classification of different NTDs.

The key contributions of this study are:

- Extracts optimal Histogram of Oriented Gradient (HOG) features by browsing the images of Buruli Ulcer (BU), Leprosy, and Cutaneous Leishmaniasis skin lesion through different basic cell sizes (CS) to obtain multiple training datasets.
- It proposes a hybrid metaheuristic algorithm combining Whale Optimization Algorithm and Shark Smell Optimization Algorithm (WOA-SSO) to optimize the Error Correcting Output Code (ECOC) framework for solving the multi-class classification problem of Support Vector Machine (SVM).
- achieves an optimized multi-class skin NTD classification with higher accuracy on the multi-channel dataset extracted from the averages of HOG features of different CS.

The results demonstrate the feasibility of developing mobile applications for early diagnosis and identification of NTDs just by taking pictures of the skin lesions, which could be utilized by frontline health workers to address isolation and poverty in combating these neglected diseases. To achieve this goal of better classification performance, this section presents the material and method of this study. It will allow us to explain the data collection, the experimental procedure, and the analysis method. Section 3 presents the results obtained, and Section 4 provides a discussion of the results.

II. MATERIALS AND METHOD

A. HOG FEATURES EXTRACTION

Image classification generally follows a number of actions (preprocessing and processing) that consist of searching for important features of the images that will serve as a dataset for learning and developing prediction models. These features can be the shape, region, and texture of the images. There are several popular feature descriptors that are commonly used in computer vision and image processing tasks such as object detection. Some of the most popular feature descriptors include:

Histogram of Oriented Gradients (HOG) is used in this study. HOG is a feature descriptor that counts occurrences of gradient orientation in localized portions of an image. It is computed on a dense grid of uniformly spaced cells and uses overlapping local contrast normalization for improved accuracy. Another widely used descriptor is Scale Invariant Feature Transform (SIFT) which identifies key points of an image that are invariant to image scaling and rotation. SIFT descriptors are highly distinctive and partially invariant to changes in illumination and 3D projection. Speeded-Up Robust Feature (SURF) is a robust feature detector that can be used for tasks such as object recognition or 3D reconstruction. It is inspired by SIFT but faster to compute. SURF uses integral images for image convolution which allows for very fast keypoint detector and descriptor extraction.

The HOG is a feature descriptor that is used in computer vision and image processing for the purpose of object detection. The technique count occurrences of gradient orientation in localized portions of an image. The method is similar to the Edge Orientation Histogram, Scale-invariant Feature Transform (SIFT) descriptors, and shape contexts. The concept was first described by Robert K. Mc Connell in 1986 [31]. Later in 2005, the usage of HOG became widespread when Navneet Dalal first introduced HOG features in his PhD thesis under Bill Triggs at French National institute for research in computer science and Automation (INRIA).

The gradient of an image or matrix depend on the row and a column surrounding it. If r is a row and c the column, we can compute de Gradient in the two directions G_x and G_y by the following relation in equation 1 and 2

$$G_x(r, c) = I(r, c + 1) - I(r, c - 1) \quad [32] \quad (1)$$

$$G_y(r, c) = I(r - 1, c) - I(r + 1, c) \quad [32] \quad (2)$$

The two main features of the HOG are the Magnitude (μ) and the rotation Angle(θ) of the pixel group I . They are computed with the equation 3 and 4.

$$\text{Magnitude } (\mu) = \sqrt{G_x^2 + G_y^2} \quad [32] \quad (3)$$

$$\text{Angle}(\theta) = \tan^{-1}\left(\frac{G_y}{G_x}\right) \quad (4)$$

For each angle we calculate the step Size ($\Delta\theta$). For example, if we divide our image in a $n \times n$ pixels group we will gate n^2 points Histogram (Bin) for each cell in the range of 0^0 to 180^0 and the step size will be

$$\Delta\theta = \frac{180}{n^2}.$$

Each i^{th} Bin will have a *boundaries* = $[\Delta\theta \cdot i, \Delta\theta \cdot (i + 1)]$. And the center of the i^{th} Bin is done by the equation 5 below.

$$C_i = \left\lfloor \frac{[\Delta\theta \cdot i + \Delta\theta \cdot (i+1)]}{2} \right\rfloor = \Delta\theta \left(i + \frac{1}{2} \right) \quad (5)$$

The steps of calculated HOG feature is given in this paragraph. For a given value of angle θ obtain from angle matrix, first we find value i and $i + 1$ wich are calculated by

$$i = \text{floor} \left(\left\lfloor \frac{\theta}{\Delta\theta} - \frac{1}{2} \right\rfloor \right).$$

Next, we assigned to i^{th} and the $(i + 1)^{th}$ Bin the value V_i (Eq.6) and V_{i+1} (Eq.7) are

$$V_i = \mu \left[\frac{C_{i+1} - \theta}{\Delta\theta} \right]. \quad (6)$$

$$V_{i+1} = \mu \left[\frac{-C_i + \theta}{\Delta\theta} \right]. \quad (7)$$

The Next step is making Overlapping Blocks from cells. Once Histogram (n^2 Bins) computation is over for all cells, then 4 cells are clubbed together to form a block. For all the four cells in block, concatenate all n^2 -point histograms of each cell to form a $4n^2$ -point feature vector, let represented as (Eq.8), $fb_i = [b_1, b_2, b_3, \dots, b_{4n^2}]$. (8)

The value of fb_i normalized by L_2 norm as shown in Eq.9,

$$fb_i \leftarrow \frac{fb_i}{\sqrt{\|fb_i\|^2}} \quad (9)$$

This normalization is done to reduce the effect of changes in contrast between images of the same object.

In the conclusion, from each $n \times n$ block, a $4n^2$ -point feature vector is collected. If in the horizontal direction we have H blocks and in the vertical one we have P blocks, therefore the total length of HOG feature is, $H \times P \times 4n^2$; and the overall extraction scheme is done by figure1 below.

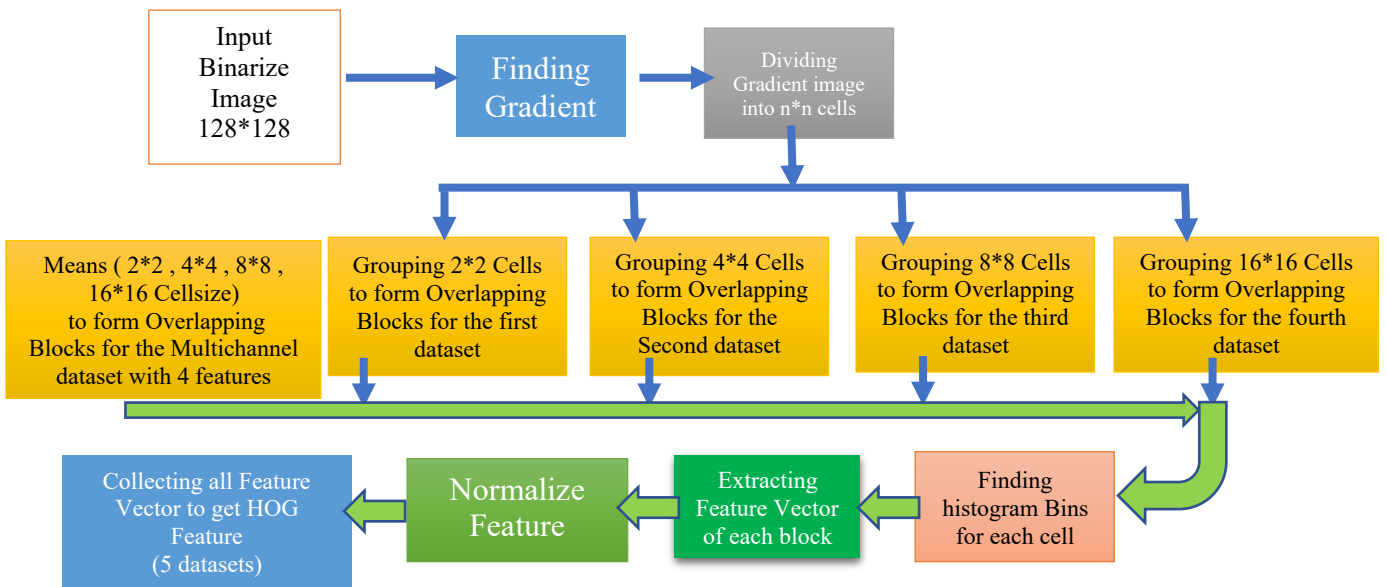


Figure 1: Overall HOG feature extraction Scheme

The output is composed of HOG feature vectors with 3 classes that we need to classify. There are several machine learning methods to do this successfully [22]. In the field of machine learning, there are many algorithms such as logistic regression and support vector machines, which are designed for two-class (binary) classification problems. Some algorithms, such as decision trees, naive Bayes, and neural networks, can handle multi-class problems directly. But these require a lot of data and hardware resources with high computational power compared to SVM. As such, these algorithms must either be modified for multi-class classification problems (more than two) or not used at all. The error-correcting output code (ECOC) method is a technique that reframes a multi-class classification problem into multiple binary classification problems, allowing native binary classification models like SVM to be used directly.

B. OPTIMIZE ECOC-SVM

Error-Correcting Output Codes (ECOC) is an ensemble method designed for multi-class classification problem. In multi-class classification problem, the task is to decide one label from $k > 2$ possible choices. ECOC is a meta method which combines many binary classifiers in order to solve the multi-class problem. Notice that in the error-correcting output code, the rows have more bits than is necessary. Using some redundant "error-correcting" bits, we can tolerate some error introduced by finite training sample, poor choice of input features, and flaws in the training algorithm. Thus, the system is more likely to recover from the errors. If the minimum Hamming distance between any pair of code words is d , then the code can correct at least

$\lfloor \frac{d-1}{2} \rfloor$ single bit errors. As long as the error moves us fewer than $\lfloor \frac{d-1}{2} \rfloor$ unit away from the true codeword, the nearest codeword is still the correct one.

There are many ways to design the error-correcting output code. Here we only introduce the two simplest ones. When the number of classes k is small ($3 < k \leq 7$), we can use exhaustive codes. Each code has length $2^{k-1} - 1$. Row 1 contains only ones. Row 2 consists of 2^{k-2} zeros followed by $2^{k-2} - 1$ ones. Row 3 consists of 2^{k-3} zeros, followed by 2^{k-3} ones, followed by 2^{k-2} zeros, followed by $2^{k-3} - 1$ ones. In [2], the authors showed that the major benefit of error-corrective coding is variance reduction via model averaging. As k increases the number of base classifiers in the ensemble increases exponentially. Hence the running time and the efficiency of the algorithm decreases. In this study we use

methods present by [23] to select the best accurate and diverse classifiers from exhaustive ECOC coding by incorporating the diversity measure Minimizing the approximate ensemble error function who is our objective function.

Consider the matrix P on the training set defined as follows: $P_{i,j} = 0$, on the j^{th} classifier is correct for point i and $P_{i,j} = 1$, else. A matrix G is then defined by the previous P values such that $G = P^T P$ with G_{ii} the total errors that the classifiers i font, make, and the diagonals G_{ij} are the errors made at position i and j . The normalized matrix is given by equations 10 and 11.

$$\tilde{G}_{ii} = \frac{G_{ii}}{N} \tag{10}$$

and

$$\tilde{G}_{ij,i \neq j} = \frac{1}{2} \left(\frac{G_{ij}}{G_{ii}} + \frac{G_{ij}}{G_{jj}} \right) \tag{11}$$

Where N represents the number of data sets. Considering the regularization constant ρ and the error ϵ , the author of [23] shows that this is an unconstrained optimization problem defined by:

$$\min_{x \in \mathbb{R}^n} x^T \tilde{G} x + \rho \|x\|_0 \tag{12}$$

With

$$\|x\|_0 := \sum_{i=1}^n 1_{x_i \neq 0} = \lim_{\epsilon \rightarrow 0} \sum_{i=1}^n \frac{\log(1+|x_i|/\epsilon)}{\log(1+\frac{1}{\epsilon})}$$

Here, the zero norm is defined by the number of non-zero elements that lead to sparsity in the model. X is the relaxation of the binary vector into a real vector, i.e., $x \in \mathbb{R}^n$. Thus, the optimization problem becomes

$$\min_{x \in \mathbb{R}^n} x^T \tilde{G} x + \rho \lim_{\epsilon \rightarrow 0} \sum_{i=1}^n \frac{\log(1+|x_i|/\epsilon)}{\log(1+\frac{1}{\epsilon})} \tag{13}$$

Here, x_i represents whether the i^{th} classifier is in the set or not. If $x_i = 1$, then it means that the i^{th} classifier is chosen to be in the set, if $x_i = 0$. Since this problem is a non-convex problem, the author adds a term to make it convex and gets the equation below.

$$\min_{x \in \mathbb{R}^n} x^T (\tilde{G} + \tau I) x - \tau \|x\|_2^2 + \rho \lim_{\epsilon \rightarrow 0} \sum_{i=1}^n \frac{\log(1+|x_i|/\epsilon)}{\log(1+\frac{1}{\epsilon})} \tag{14}$$

Where $\| \cdot \|_2$ refers to the Euclidean norm. This function will be used as a cost function for the ECOC classification. This equation can be solved by metaheuristics. The minimization algorithm inspired by [23] is given by the following pseudocode.

Algorithm Optimized ECOC Framework

Input: a k class problem, Base classifier, ECOC matrix $M_{k \times n}$

Output: error rates of test Set

- 1: Partition data X into Training Set X_{tr} and Test X_{test}
- 2: Run base classifier for each column of $M_{k \times n}$ on X_{tr}
- 3: Compute the matrix \tilde{G}
- 4: Compute a solution x with metaheuristic Algorithm for equation 14

$$\min_x x^T (\tilde{G} + \tau I)x - \tau \|x\|_2^2 + \rho \sum_{i=1}^n \frac{\log(1 + \frac{|x_i|}{\epsilon})}{\log(1 + \frac{1}{\epsilon})}$$

- 5: Find all i 's such that $x_i \geq 0.5, i = 1 \dots m$ to be the indices of new classifiers in subsets
- 6: Construct new ECOC matrix $M_{k \times m}$ by choosing columns from indices in step 5.
- 7: Run ECOC framework with \tilde{M} on test set X_{test}

Figure 2: Optimize ECOC Framework pseudocode

In the literature, single-objective optimization (minimization or maximization) problems are wonderfully solved by metaheuristics [24–26]. Thus, to solve equation 14, we use a hybrid metaheuristic algorithm combining the Whale optimization algorithm and Shark Smell optimization algorithm (WOA-SSA). The modeling of this algorithm is given below.

Whale Optimization Algorithm (WOA)

The WOA algorithm is inspired by the hunting technic used by humpback whale who create bubble nets to trap their prey. This method consists of two phases: the exploration phase and the exploitation phase mathematically modelled by equations 14 to 20:

Exploration Phase:

$$D = |C * X_{rand}(t) - X(t)| \tag{14}$$

$$X(t + 1) = (X_{rand}(t) - A * D) \tag{15}$$

$$a = 2 - \frac{2t}{t_{max}} \tag{16}$$

$$A = 2 * a * r - a \tag{17}$$

$$C = 2 * r \tag{18}$$

Exploitation Phase:

$$X(t + 1) = \begin{cases} D' * e^{bl} * \cos(2\pi l) + X^*(t), & p \geq 0.5 \\ X^*(t) - A * D, & p < 0.5 \end{cases} \tag{19}$$

$$D' = |X^*(t) - X(t)| \tag{20}$$

The paragraph below presents the Shark Optimization Algorithm.

Shark Smell optimization Algorithm.

The Shark Smell Optimization Algorithm is a population-based metaheuristic that is inspired by shark Food forging behavior characterize by his sense of smell. His strategy is based on forward movement and rotational movement with a certain velocity. The modelling of the two behavior is done by Eq.21 and Eq.22 below.

$$Y_i^{k+1} = X_i^k + V_i^k \Delta t_k \tag{21}$$

This equation calculates the position based on the forward motion of the shark. Then another equation models the ability to turn around the prey, with k the current iteration, V the velocity; X is the position; i the individual shark and Y is Forward position; Here we consider $\Delta t_k = 1$ and $R =$ random number the new position taking in account the rotational behavior is given by equation 15 below

$$Z_i^{k+1} = Y_i^{k+1} + R * Y_i^{k+1} \tag{22}$$

Hybridization of Shark Smell Algorithm and Whale Optimization Algorithm to train weights of Neural Networks

The hybridization here is to combine the trapping ability of the whale in creating a giant bubble net with the speed and precision of the shark in its forward propagation phase. This is

mathematically modelled by merging Eq.19 and Eq.20 in the exploitation phase as follows.

$$X(t + 1) = \begin{cases} D' * e^{bl} * \cos(2\pi l) + X^*(t), & p \geq 0.5 \\ X^*(t) - A * D, & p < 0.5 \end{cases} \quad (23)$$

With

$$D'_i^k = \begin{cases} X^*(t) - Y_i^k(t) \\ X^*(t) - X_i^k(t) + V_i^k(t)\Delta t_k \end{cases} \quad (24)$$

C. DATASET

The images used are photographic images from various databases. <https://doi.org/10.35078/1PSIEL> [13] was used to obtain a portion of the leprosy images (2/3) Another part was obtained from the study of [3]. The rest of the images were obtained from the DermNet platform, the world's leading free dermatology resource. All images followed the minimum requirements of the International Skin Imaging Collaboration (ISIC), including background color, illumination, field of view, focus/depth of field, resolution, scaling, and color calibration. The set consists of 3000 images distributed according to Figures 3, 4, and 5.

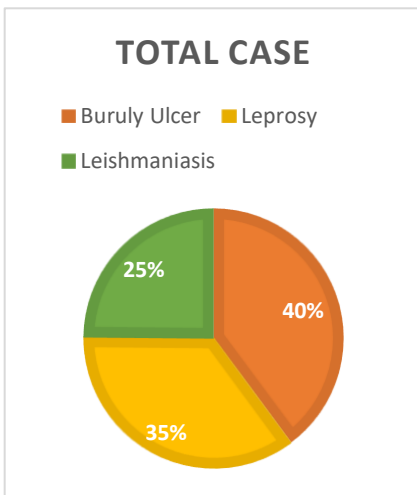


Figure 3: Entire Datasets

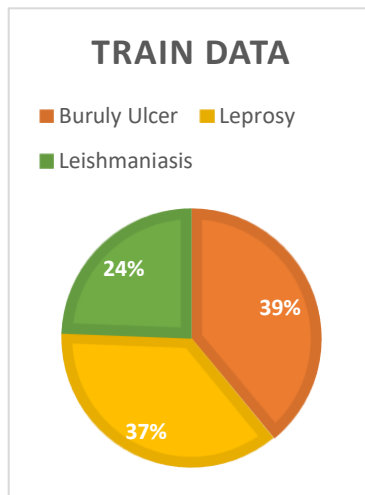


Figure 4: Train dataset

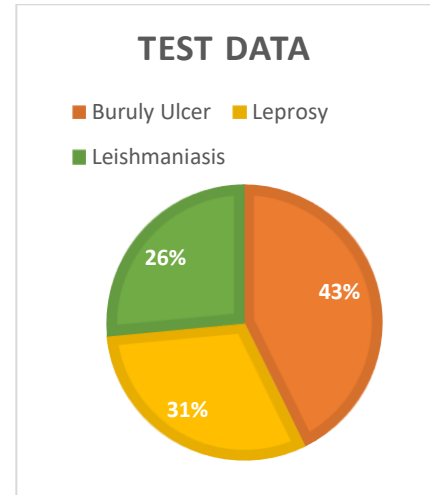


Figure 5: Train dataset

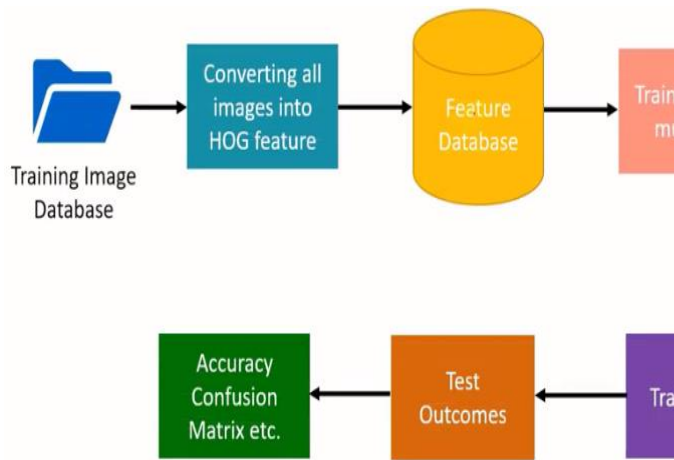
These figures show that the images are more or less balanced in number. For the following, the images are divided into training data (2400) and test data (600). All images are 128*64 in size and in grayscale form.

D. EXPERIMENTAL PROCEDURES

The experimentation will be done according to figure 6. We convert our images into HOG features, which constitute our

training basis. We will obtain four datasets that will serve as our training data.

Then, we train our data using a hybrid WOA-SSO-ECOC-SVM algorithm, which provides us with an intelligent model to which we can apply our test images and estimate performance metrics



Consider our 3 classes, we will have 3 columns and 4 rows. The first row contains four 1's. The second row contains two 0's followed by two 1's. The last row contains alternating values of 0 and 1 respectively. Figure 7 shows the ECOC classification process. We have two inputs consisting of the HOG features extracted from the images and the ECOC coding matrix of the classes. The binary outputs of the SVMs are used to construct a binary number to be compared with the codes of the ECOC matrix. The error matrix G is formed and minimized by our metaheuristic.

Figure 6:

Overall classification Scheme

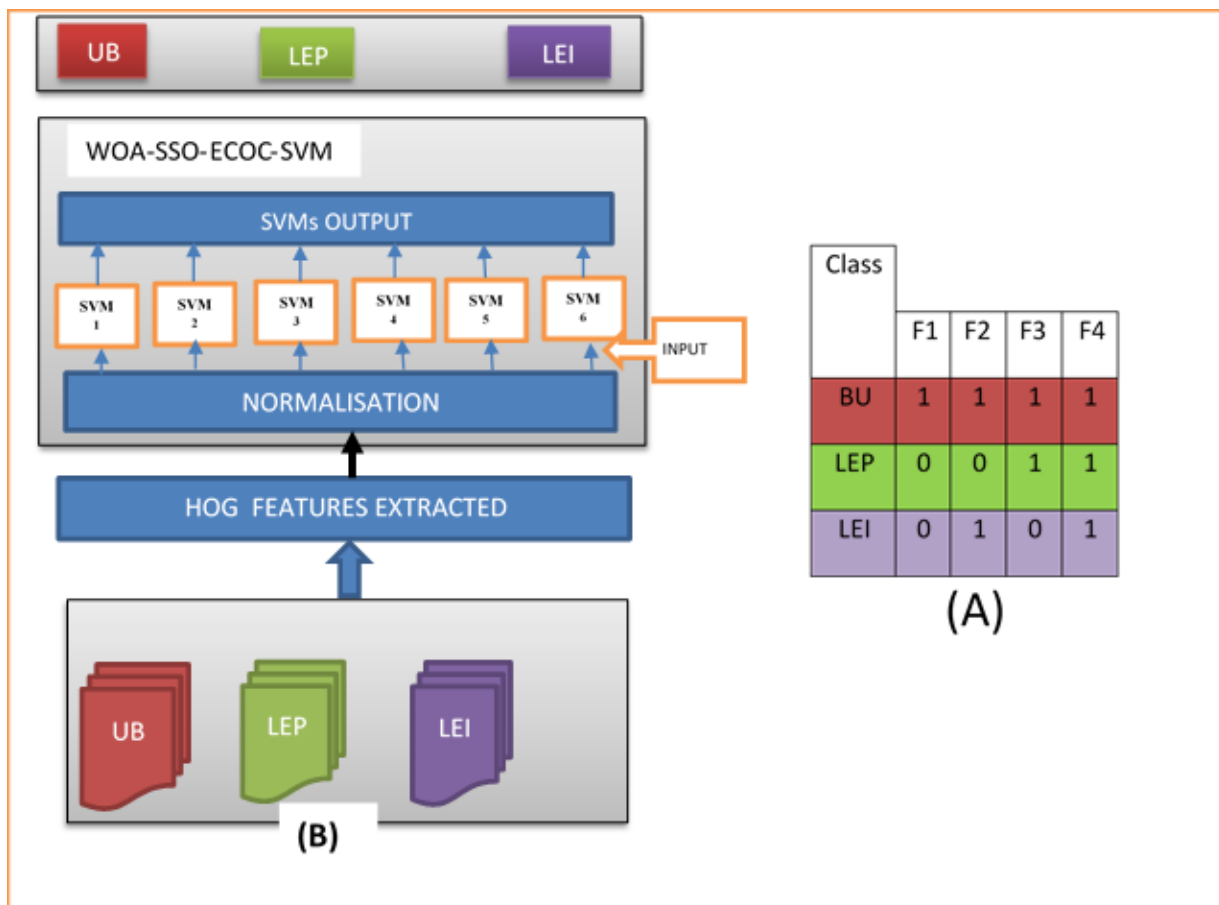


Figure 7: (B) ECOC SVM Architecture; (A) Binary ECOC for a 3-class Problem

The diagnostic algorithm is presented in the following figure 8. We first divide our database into three sets: a training set,

a test set, and a test validation set. Then we read all the images to extract features for training.

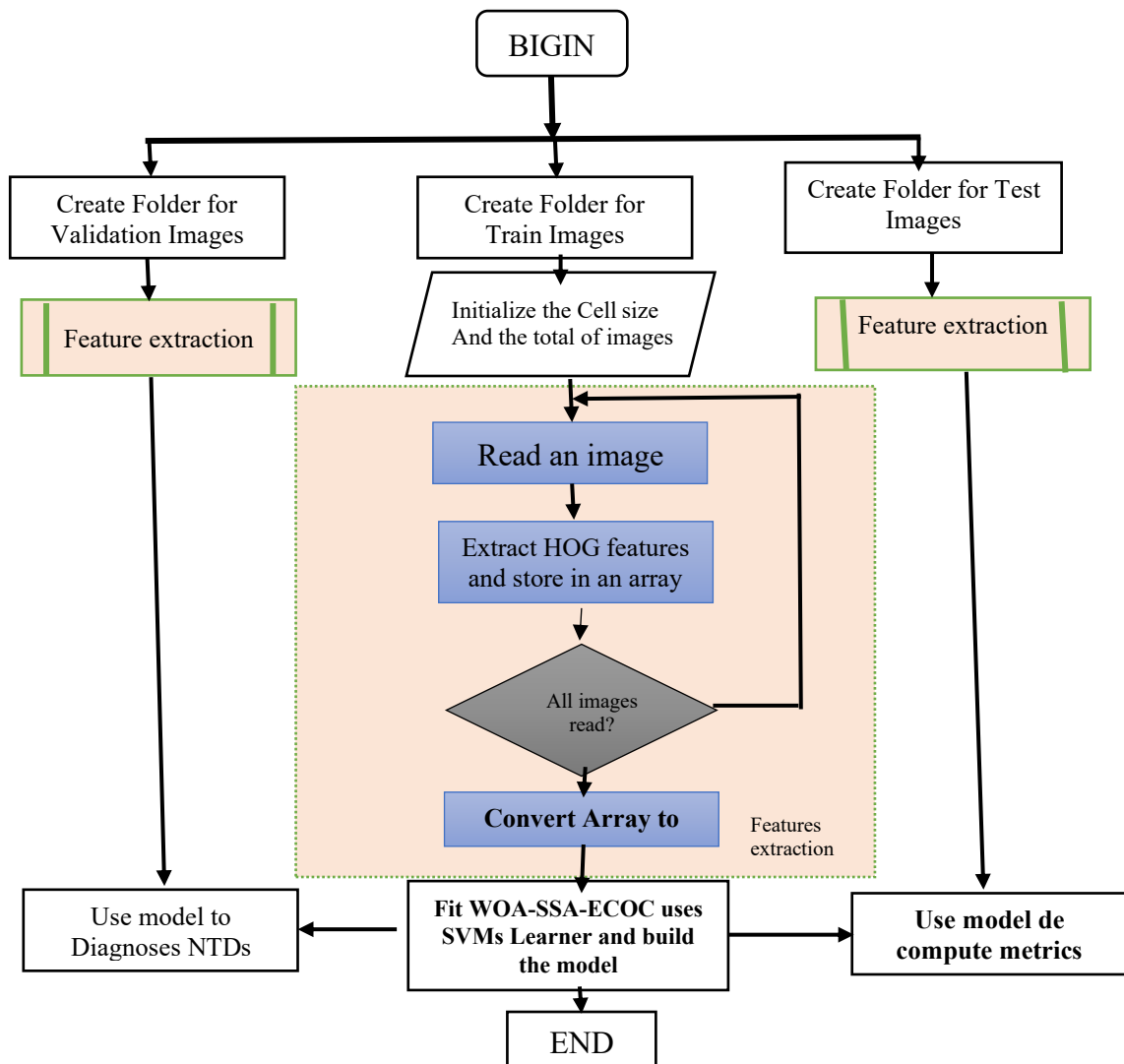


Figure 8: Classification and diagnostic process

Our problem is a multi-class classification problem. From the confusion matrix, we determine the following metrics:

Accuracy, mean error, MSE, RMSE and error STD. The following section presents the different results obtained. The results will be given in percentage.

III. RESULT

A. HOG FEATURES EXTRACTED

We apply our extraction algorithm to different basic cell sizes (CS) and we obtain 4 datasets corresponding to the sizes Cellsize = [2 2], Cellsize = [4 4], Cellsize = [8 8], Cellsize = [16 16], and a multichannel dataset corresponding to the averages of the first four HOG

features $X = [\text{mean}(\text{Cellsize} = [2\ 2]), \text{mean}(\text{Cellsize} = [4\ 4]), \text{mean}(\text{Cellsize} = [8\ 8]), \text{mean}(\text{Cellsize} = [16\ 16])]$ which allows us to have 5 datasets as presented in figure 9 below. We have to choose the one that gives the best results. After analysis of the data, the dataset with the best results is the multichannel one made up of the averages of the first four datasets, and the worst dataset is the one resulting from the cellsize 2*2.

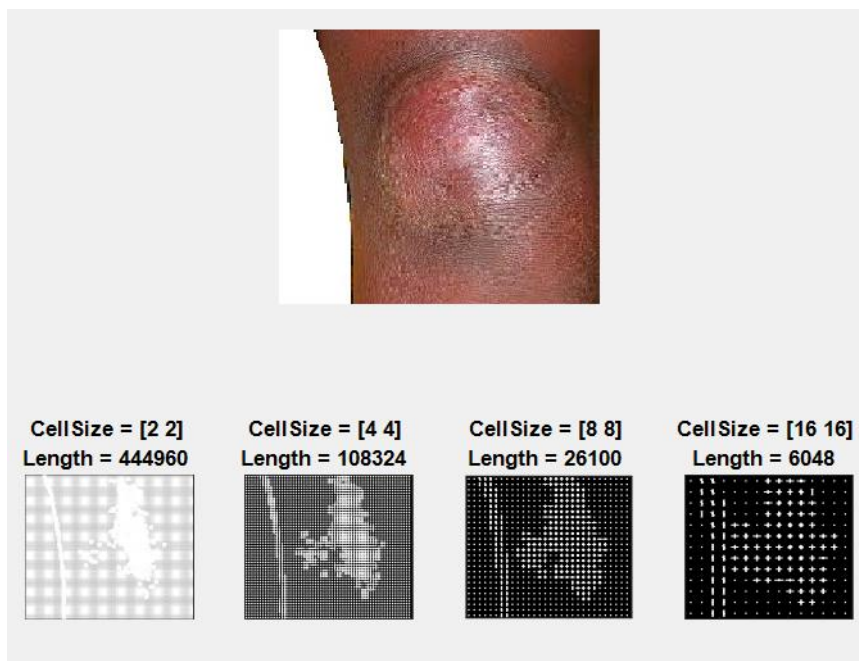


Figure 9: Different treatments according to the cell sizes

Figures 10, 11, 12, and 13 show the classification error values on a validation set of 60 data points from various classes. As we can see above each image, there are error values in terms of MSE, RMSE, Error Mean, and Error STD. We can see that

it is the multichannel dataset that has better results in most of the metrics except for the mean error, which is smaller on the CS4*4 dataset. This allows us to validate this dataset as optimal for our study.

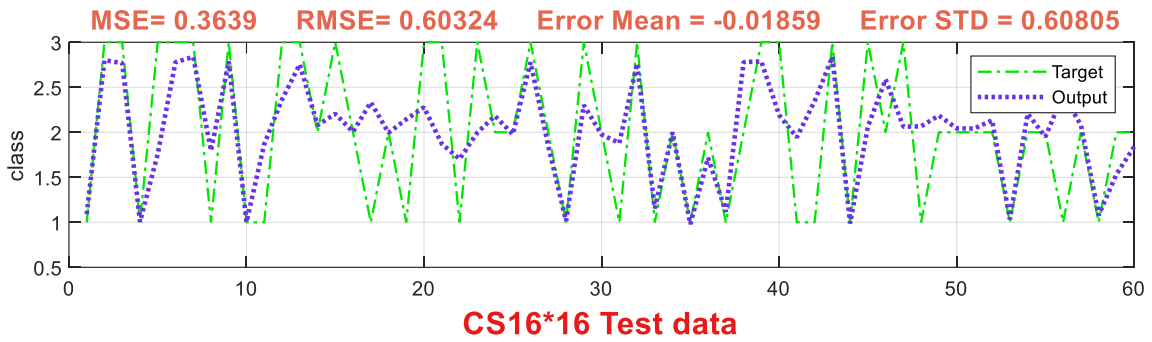


Figure 10: Classification of test data from the cellsize 16*16.

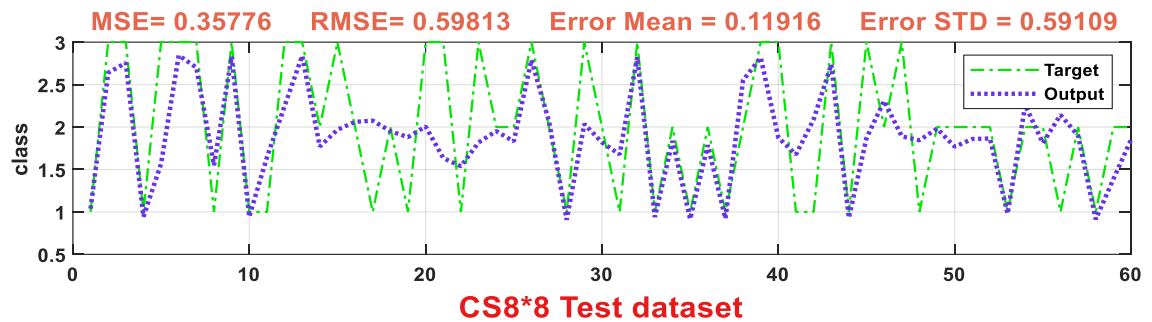


Figure 11: Classification of test data from the cellsize 8*8.

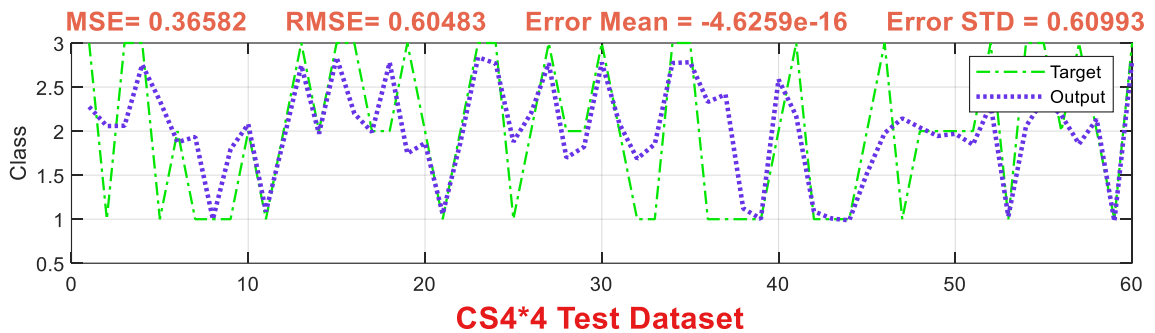


Figure 12: Classification of test data from the cellsize 4*4.

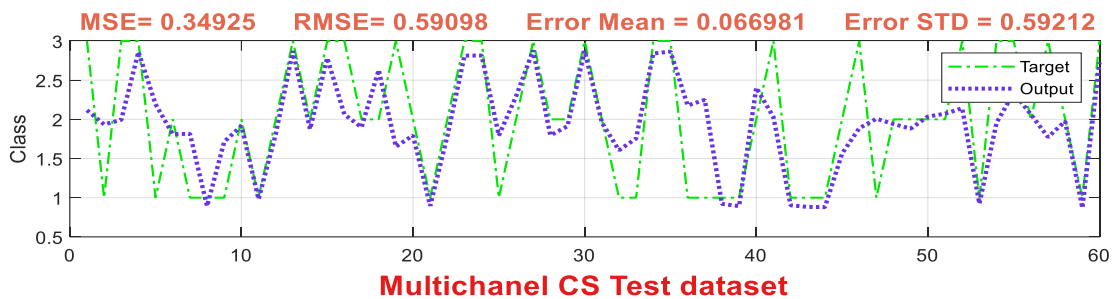


Figure 13: Classification of test data from multi-channel data

The results indicate that the multi-channel dataset outperforms individual cell size datasets in terms of accuracy and error metrics. The multi-channel dataset achieves an accuracy of

84.69%, significantly higher than the accuracy obtained using individual cell size datasets (72.9667% for CS 44, 72.9667% for CS 88, and 78.9667% for CS 16*16). This suggests that

combining information from different cell sizes enhances the discriminative power of the features and improves the classification performance. Furthermore, the multi-channel dataset exhibits consistently superior performance across various error metrics, including Mean Squared Error (MSE), Root Mean Squared Error (RMSE), Error Standard Deviation (Error STD), and accuracy. This consistency indicates the robustness and reliability of the proposed method.

The lower MSE and RMSE values for the multi-channel dataset indicate that the model is able to predict the actual values more accurately, resulting in smaller errors. The lower

Error STD value suggests that the model's predictions are less variable and more consistent. Overall, the results demonstrate the effectiveness of the multi-channel HOG feature extraction approach and the hybrid metaheuristic algorithm optimization in improving the accuracy of NTD diagnosis. The superior performance of the multi-channel dataset and the consistent results across multiple evaluation metrics highlight the potential of this method for revolutionizing NTD diagnosis and management. Table 2 summarizes the statistical values for the four datasets under study. It confirms the best results obtained on the multi-channel dataset.

Table 2. Various errors obtained after classification of the data in our datasheets

	MSE	RMSE	Error Mean	%Error standard	Accuracy
CellSize 4*4 Dataset	0.36582	0.60483	-4.625e-16	0.60993	72.9667
CellSize 8*8 Dataset	0.35776	0.59813	0.11916	0.59109	72.9667
CellSize 16*16 Dataset	0.3639	0.6034	-0.01859	0.60805	78.9667
Multichannel CellSize Dataset	0.34925	0.59093	0.066981	0.59212	84.69%

As said above, the best results in terms of MSE and RMSE, and the confusion matrices present accuracy values of 72.9667% Error STD are obtained from the multichannel data from the line for CS 4*4, 72.9667% for CS 8*8, 78.9667% for CS 16*16, 84% averages of the other data sets. This result is validated by the accuracy values obtained on one test set. As can be seen in Figure

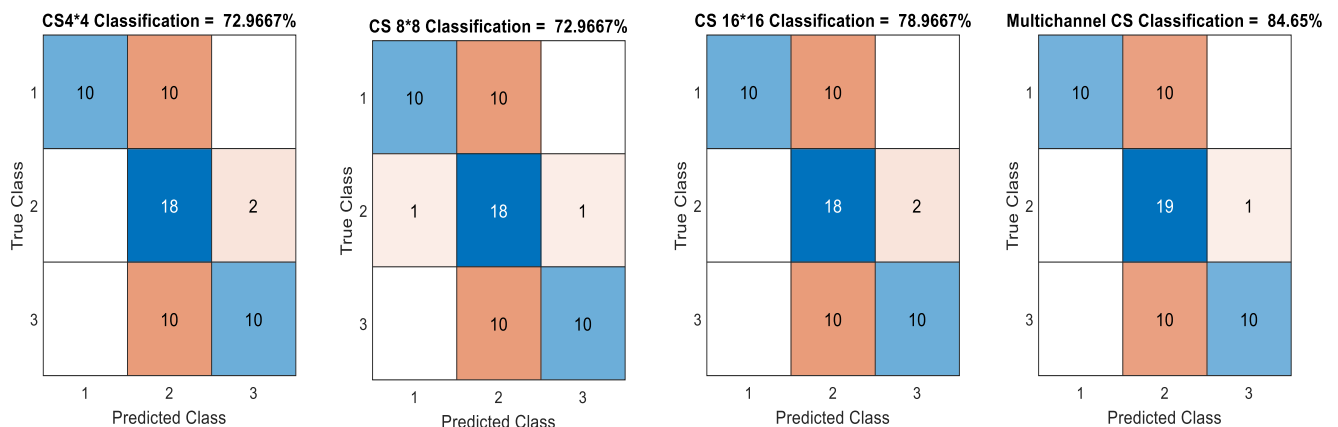


Figure 14: Classification of test data from different databases

B. OPTIMIZE ECOC-SVM

Having chosen our optimal dataset, we compare in this paragraph our optimized ECOC-SVM algorithm and the non-optimized one on the multichannel database. Figure 15 shows the learning process of the two algorithms. The analysis of the

optimized and non-optimized ECOC-SVM algorithms on the multichannel dataset is a crucial step in evaluating the effectiveness of the optimization process.

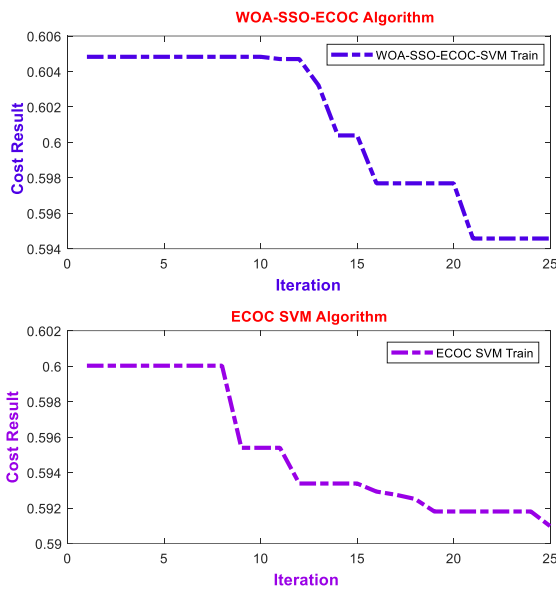


Figure 15: Optimized and non-optimized ECOC learning process
As can be seen, the optimized algorithm seems to converge slowly from the 13th iteration and, around the 20th iteration, converges quickly to stabilize. On the other hand, the non-optimized algorithm seems to converge quickly from the 8th iteration, but its minimum remains lower than the optimized one. These results are summarized in the following table 3.

Table 3. Comparison of the results between the optimized and non-optimized algorithms

Algorithm	Min lost	Iteratio n	accurac y
ECOC SVM	0.5948	25	84.69
WOA-SSO-ECOC-SVM	0.5951	21	89.77

The provided results indicate that the WOA-SSO-ECOC-SVM algorithm outperforms the standard ECOC-SVM algorithm in terms of both loss and accuracy.

Key Observations:

- **Lower Loss:** The WOA-SSO-ECOC-SVM algorithm achieves a minimum loss of 0.5951, compared to 0.5948 for the standard ECOC-SVM algorithm. This suggests that the WOA-SSO optimization process effectively improves the model's ability to minimize the difference between predicted and actual values.
- **Higher Accuracy:** The WOA-SSO-ECOC-SVM algorithm achieves an accuracy of 89.77%, significantly higher than the 84.69% accuracy

achieved by the standard ECOC-SVM algorithm. This indicates that the optimization process leads to a more accurate classification model, reducing the number of misclassified instances.

- **Faster Convergence:** The WOA-SSO-ECOC-SVM algorithm converges to its optimal solution in 21 iterations, while the standard ECOC-SVM algorithm requires 25 iterations. This suggests that the WOA-SSO optimization process enhances the model's convergence speed, reducing the computational time required for training.

Implications:

- **Improved NTD Diagnosis:** The superior performance of the WOA-SSO-ECOC-SVM algorithm in terms of loss and accuracy has significant implications for NTD diagnosis. The higher accuracy translates to a lower rate of misdiagnosis, potentially improving patient outcomes and reducing the spread of these diseases.
- **Enhanced Computational Efficiency:** The faster convergence of the WOA-SSO-ECOC-SVM algorithm makes it more suitable for real-time applications, where timely diagnosis is crucial. This could facilitate the development of mobile applications for NTD diagnosis, enabling rapid and accurate diagnosis in resource-limited settings.
- **Revolutionizing NTD Management:** The improved accuracy and efficiency of the WOA-SSO-ECOC-SVM algorithm hold promise for revolutionizing NTD management. By enabling earlier and more accurate diagnosis, this approach could contribute to improved disease control, reduced morbidity and disability, and ultimately, improved public health outcomes.

IV. DISCUSSION

This study allowed us to validate that by associating several HOG features from several cellsize images, we extract the best parameters in order to optimize the classification accuracy. This is because by combining these features, we recover information that we would have lost if we used a single cellsize. The results obtained after classification of our optimal database and classification by ECOC-SVM optimized allow us to have better results in terms of accuracy.

However, this result is not very bad compared to the literature and the diagnostic methods frequently used to diagnose these diseases. For example, the Direct smear examination and In vitro culture methods all have sensitivities of less than 60% [27]. These works are summarized in the table 4 below.

Table 4. Comparison with results from literature

Author	Lesion type			Dataset		
	Buruli ulcer	Leishmaniasis	Leprosy	Images	Clinical data	Accuracy
Rui Hu et al [15]	YES	NO	NO	26	NO	85.70%
Márcio Luís Moreira [21]	NO	YES	NO	300	NO	50%
Direct smear examination [27]	YES	YES	YES			<60%
In vitro culture [27]	YES	YES	YES			20-60%

The probable reasons why we have an accuracy lower than 90% are due to the extracted HOG features. In general, they are used for face recognition tasks and shapes in general [28] [29] [30]. On the other hand, our images do not really have contests of very accentuated shapes, like a human face, the shape of an animal, or an object. This study allows us to consider the development of a computer-aided-diagnosis to diagnose neglected tropical diseases in their initial phase.

The study on multi-class classification of neglected tropical skin diseases using multi-channel HOG features presents several limitations and implications. The limited data size and diversity might restrict the generalizability of the proposed method. The computational complexity of the hybrid metaheuristic algorithm could pose challenges for real-time applications. Additionally, the study's focus on three specific diseases raises questions about its applicability to other skin conditions. Furthermore, the lack of validation on external datasets limits the assessment of the model's generalizability and robustness.

Despite these limitations, the study holds significant implications for improving healthcare access and outcomes. Mobile applications based on the proposed method could facilitate early diagnosis and treatment, particularly in remote areas with limited access to healthcare facilities. This could potentially reduce the burden on healthcare systems and improve patient outcomes. However, further research is needed to address the limitations and validate the method's effectiveness on a broader scale.

V. CONCLUSION

The aim of our study was to show that HOG features can be potential candidates for the classification of skin lesions. For this purpose, we extracted from photographic images skin lesions of three neglected tropical diseases in their early phase. After having extracted HOG features by browsing the images by cells of "bases of size 2*2, 4*4, 8*8 and 16*16, we obtained 4 datasets, which unfortunately gave poor precision in the classification. But by combining the four datasets into one, each cell of a column being the average of the rows of each

dataset, we obtain an optimal dataset with better accuracy. In order to do a multi-class classification, we used the ECOC Framework optimized to allow one VS one classifications. The results obtained prove that the features extracted from the averages of the other features have better results in terms of error and percentiles. Thus, our Multi Channel CellSize Dataset obtained an MSE of 0.34925, an RMSE of 0.59093, an average error of 0.066981, an STD error of 0.5921 and an Accuracy of 89.77%. As we said in the section talking about the limitations of this study, this classification rate is not very good and we are thinking of adding to the shape features (HOG) other texture features like LGCMs in our future work.

ACKNOWLEDGMENT

We thank the anonymous reviewers for their insightful comments and suggestions, which helped us improve the quality of this manuscript.

REFERENCES

- [1]. World Health Organization. (2018). [Recognizing neglected tropical diseases through changes on the skin: a training guide for front-line health workers](#)
- [2]. Reithinger, R., Dujardin, J. C., Louzir, H., Pirmez, C., Alexander, B., & Brooker, S. (2007). Cutaneous leishmaniasis. *The Lancet infectious diseases*, 7(9), 581-596.
- [3]. Sakyi, S. A., Aboagye, S. Y., Darko Otchere, I., & Yeboah-Manu, D. (2016). Clinical and laboratory diagnosis of Buruli ulcer disease: a systematic review. *Canadian Journal of Infectious Diseases and Medical Microbiology*, 2016.
- [4]. Rahman, M. M., Nasir, M. K., Nur, A., Khan, S. I., Band, S., Dehzangi, I., ... & Rokny, H. A. (2022). Hybrid Feature Fusion and Machine Learning Approaches for Melanoma Skin Cancer Detection.
- [5]. Bansal, P., Garg, R., & Soni, P. (2022). Detection of melanoma in dermoscopic images by integrating features extracted using handcrafted and deep learning models. *Computers & Industrial Engineering*, 168, 108060.
- [6]. Bansal, P., Vanjani, A., Mehta, A., Kavitha, J. C., & Kumar, S. (2022). Improving the classification accuracy of melanoma detection by performing feature selection using binary Harris hawks optimization algorithm. *Soft Computing*, 26(17), 8163-8181.
- [7]. Kamil, M. Y. (2022). Evaluation of Machine Learning Models for Breast Cancer Diagnosis Via Histogram of Oriented Gradients Method and Histopathology Images. *International Journal on Recent*

and Innovation Trends in Computing and Communication, 10(4), 36-42.

[8]. Mishra, A. K., Roy, P., Bandyopadhyay, S., & Das, S. K. (2022). Feature fusion based machine learning pipeline to improve breast cancer prediction. *Multimedia Tools and Applications*, 1-29.

[9]. Alyami, J., Khan, A. R., Bahaj, S. A., & Fati, S. M. (2022). Microscopic handcrafted features selection from computed tomography scans for early stage lungs cancer diagnosis using hybrid classifiers. *Microscopy Research and Technique*.

[10]. SureshKumar, M., Dahiya, D., Shanmugapriya, P., & ReneRobin, C. R. (2022). Integrated Global and Local Feature Extraction and Classification from Computerized Tomography (CT) Images for Lung Cancer Classification.

[11]. Shetty, A., Shah, K., Reddy, M., Sanghvi, R., Save, S., & Patel, Y. (2022). Skin Cancer Detection Using Image Processing: A Review. In *Proceedings of the 2nd International Conference on Recent Trends in Machine Learning, IoT, Smart Cities and Applications* (pp. 103-121). Springer, Singapore.

[12]. Barati, E., Saraee, M. H., Mohammadi, A., Adibi, N., & Ahmadzadeh, M. R. (2011). A survey on utilization of data mining approaches for dermatological (skin) diseases prediction. *Journal of Selected Areas in Health Informatics (JSHI)*, 2(3), 1-11.

[13]. Barbieri, R. R., Xu, Y., Setian, L., Souza-Santos, P. T., Trivedi, A., Cristofono, J., ... & Moraes, M. O. (2022). Reimagining leprosy elimination with AI analysis of a combination of skin lesion images with demographic and clinical data. *The Lancet Regional Health-Americas*, 9, 100192.

[14]. HU, Rui, QUEEN, CourtneyM, et ZOURIDAKIS, George. A novel tool for detecting Buruli ulcer disease based on multispectral image analysis on handheld devices. In : *IEEE-EMBS International Conference on Biomedical and Health Informatics (BHI)*. IEEE, 2014. p. 37-40.

[15]. ZARE, Mojtaba, AKBARIALIABAD, Hossein, PARSAEI, Hossein, et al. A machine learning-based system for detecting leishmaniasis in microscopic images. *BMC Infectious Diseases*, 2022, vol. 22, no 1, p. 1-6.

[16]. BAMOROVAT, Mehdi, SHARIFI, Iraj, RASHEDI, Esmat, et al. A novel diagnostic and prognostic approach for unresponsive patients with anthroponotic cutaneous leishmaniasis using artificial neural networks. *PLoS One*, 2021, vol. 16, no 5, p. e0250904.

[17]. De Souza MLM et al. "Leprosy Screening Based on Artificial Intelligence: Development of a Cross-Platform App" *JMIR Mhealth Uhealth* 2021.

[18]. Agliari, E., Alemanno, F., Barra, A., & De Marzo, G. (2022). The emergence of a concept in shallow neural networks. *Neural Networks*, 148, 232-253.

[19]. Birzhandi, P., Kim, K. T., & Youn, H. Y. (2022). Reduction of training data for support vector machine: a survey. *Soft Computing*, 26(8), 3729-3742.

[20]. Xiong, X., Hu, S., Sun, D., Hao, S., Li, H., & Lin, G. (2022). Detection of false data injection attack in power information physical system based on SVM-GAB algorithm. *Energy Reports*, 8, 1156-1164.

[21]. Zhou, T., Dou, H., Tan, J., Song, Y., Wang, F., & Wang, J. (2022). Small dataset solves big problem: An outlier-insensitive binary classifier for inhibitory potency prediction. *Knowledge-Based Systems*, 251, 109242.

[22]. Singh, A., Thakur, N., & Sharma, A. (2016, March). A review of supervised machine learning algorithms. In *2016 3rd International Conference on Computing for Sustainable Global Development (INDIACom)* (pp. 1310-1315). Ieee.

[23]. Özögür-Akyüz, S., Windeatt, T. & Smith, R. Pruning of Error Correcting Output Codes by optimization of accuracy-diversity trade off. *Mach Learn* **101**, 253-269 (2015). <https://doi.org/10.1007/s10994-014-5477-5>

[24]. Rastgoufard, S., & Charalampidis, D. (2016, October). Parameter selection of multi-class SVM with evolutionary optimization methods for static security evaluation in power systems. In *2016 IEEE Electrical Power and Energy Conference (EPEC)* (pp. 1-6). IEEE.

[25]. Krishna, G. S., & Prakash, N. (2021). A new training approach based on ECOC-SVM for SAR image retrieval. *International Journal of Intelligent Enterprise*, 8(4), 492-517.

[26]. Merdivan, E. (2013). *Optimising ECOC matrices in multi-class classification problems* (Doctoral dissertation).

[27]. Herbinge, K. H., Adjei, O., Awua-Boateng, N. Y., Nienhuis, W. A., Kunaa, L., Siegmund, V., ... & Bretzel, G. (2009). Comparative study of the sensitivity of different diagnostic methods for the laboratory diagnosis of Buruli ulcer disease. *Clinical Infectious Diseases*, 48(8), 1055-1064.

[28]. Tan, H., Yang, B., & Ma, Z. (2014). Face recognition based on the fusion of global and local HOG features of face images. *IET computer vision*, 8(3), 224-234.

[29]. Xiang, Z., Tan, H., & Ye, W. (2018). The excellent properties of a dense grid-based HOG feature on face recognition compared to Gabor and LBP. *IEEE Access*, 6, 29306-29319.

[30]. Li, X. Y., & Lin, Z. X. (2017, October). Face recognition based on HOG and fast PCA algorithm. In *The Euro-China Conference on Intelligent Data Analysis and Applications* (pp. 10-21). Springer, Cham.

[31]. McConnell, R. K. (1986). U.S. Patent No. 4,567,610. Washington, DC: U.S. Patent and Trademark Office.

[32]. Rahmawaty, M. (2021). Modeling, Simulation, and Stabilization of a Two-Wheeled Inverted Pendulum Robot Using Hybrid Fuzzy Control. *Indonesian Journal of electronics, electromedical engineering, and medical informatics*, 3(3), 93-98.



Dr NYATTE STEYVE

Dr NYATTE STEYVE is an Assistant Professor in the Computer Science and Engineering department at the University of Douala, Cameroon. He holds a PhD in Computer Science and Artificial Intelligence and has over 15 publications in renowned peer-reviewed national and international journals and conferences. His research interests lie in Data Mining, Optimization, Machine Learning, Cloud Computing, and Artificial Intelligence. Dr NYATTE STEYVE's expertise in these domains makes him a valuable asset to the University of Douala and the broader research community. He is actively involved in various research projects related to artificial intelligence applications in agriculture, healthcare, and education. His contributions to these projects have led to the development of innovative solutions that address real-world challenges.



Dr NYATTE STEYVE is a passionate educator and mentor. He is dedicated to fostering the next generation of computer scientists and engineers by providing them with the knowledge and skills necessary to thrive in the rapidly evolving field of artificial intelligence.

Contact:

Email: steyve@gmail.com

Pr STEVE PERABI NGOFFE

Pr STEVE PERABI NGOFFE is a renowned expert in mechanical engineering and control systems at the University of Douala in Cameroon. His skills and expertise encompass a wide range of areas, including hybrid systems, photovoltaics, material modeling, electrical power engineering, power electronics, power converters, inverters, power microgrids, optimization, maintenance, electrical equipment and machinery, electrical and electronic engineering, transformers, power system stability, voltage regulation, and electrical protection. Pr NGOFFE is an active researcher and has published 34 research articles on ResearchGate. His expertise and experience make him a valuable asset to the development of the energy and industrial sectors in Cameroon.

Pr SALOMÉ NDJAKOMO ESSIANE

Pr Salomé Ndjakomo Essiane is a prominent figure in the field of electrical engineering and renewable energies in Cameroon. She currently holds the positions of Director of HTTTC (Higher Technical Teacher Training College) and Head of Department at the University of Douala/University of Ebolowa. Her expertise and skills include electrical engineering, power systems simulation, MATLAB simulation, electrical & electronics engineering, renewable energy technologies, power electronics, power systems modeling, and harmonics. She has actively published 75 research articles on ResearchGate, demonstrating her significant contributions to the field. You can reach her at salomendjakomo@gmail.com. Pr Ndjakomo Essiane's expertise, experience, and research activity make her a valuable asset to the development of the energy sector in Cameroon.



Pr ELE PIERRE Pr Pierre Ele is a renowned expert in image processing and data compression., he possesses extensive expertise in the following areas: neuro-fuzzy, compression, data compression, and image processing. Pr Ele is an active researcher and has published 70 research articles on ResearchGate, demonstrating his significant contributions to these fields. His expertise and experience make him a valuable asset for the development of innovative technologies in the field of image processing and data compression.

MEPOULI KEDY. received the B.S. degree in engineering from Tunisia, and the M.S. degree in Electrotechnic, Electronics, Automatic and Telecom from the University of Douala, in 2021. He is currently pursuing the Ph.D. degree in EEAT at University of Douala. From 2020 to 2024, he was a Research Assistant with the University Institute Of Technology Douala. His research interest includes the development maintenance of biomedical devices using artificial intelligence.

